THE JOURNAL OF PHYSICAL CHEMISTRY C LETTERS

2008, *112,* 8499–8506
Published on Web 05/16/2008

Characterization of Thermally Reduced Graphene Oxide by Imaging Ellipsometry

Inhwa Jung,[†] Matthias Vaupel,[‡] Matthew Pelton,[§] Richard Piner,[†] Dmitriy A. Dikin,[||] Sasha Stankovich,[||] Jinho An,[†] and Rodney S. Ruoff*[,†]

Department of Mechanical Engineering, The University of Texas at Austin, Austin, Texas, 78712, Nanofilm Technologie GmbH, Anna-Vandenhoeck-Ring 5, Göttingen, 37081 Germany, Center for Nanoscale Materials, Argonne National Laboratory, Argonne, Illinois 60439, and Department of Mechanical Engineering, Northwestern University, Evanston, Illinois 60208

Received: March 12, 2008; Revised Manuscript Received: April 28, 2008

The dispersion functions for the refractive index and the extinction coefficient of single- and multiple-layer graphene oxide samples were measured by imaging spectroscopic ellipsometry in the wavelength range of 350−1000 nm and were compared to previously reported results measured by confocal microscopy. The dispersion functions for thin platelets were also compared to those obtained by standard spectroscopic ellipsometry on a deposit consisting of many overlapping graphene oxide layers. Changes were observed in both the thickness of the deposits and the values of the dispersion parameters following heating. A model is proposed to explain these observations, based on the removal of water between the graphene-oxide layers upon thermal treatment.

Introduction

Graphene is an atomically thin carbon nanostructure, which has recently attracted a great deal of attention as a potential novel electronic material, due to its unique transport properties.[1,2] Commonly used techniques of mechanical exfoliation yield a very small fraction of single graphene layers. Chemical exfoliation has thus recently been applied as an alternative method to obtain a large number of single layers.[3–5] This method produces heavily oxidized layers, referred to as graphene oxide, which contain a large number of epoxide and hydroxyl groups within the graphene structure. These functional groups can be partially removed by reduction techniques, yielding a partially reduced structure that is of interest as a filler for nanocomposites,[6,7] as the main component of a paper-like material,[8,9] and as a potential nanoelectronic material.[10,11] Thin films composed of reduced graphene oxide sheets have also been suggested for novel transparent conducting films,[12,13] which may play an important role, for example, as conductive layers in future low-cost photovoltaics.

Because the optical properties of the material are sensitive to its oxygen content, they can provide an important probe of its properties. Films based on graphene oxide or on modified graphene oxide are of interest for applications where the optical properties are central to performance, such as for transparent conductive films; it is therefore important to characterize optical properties of individual platelets. However, it is not straightforward to detect and measure the optical properties of a single layer of graphene-based material, due to its small thickness (less than 1 nm) and limited lateral dimensions (typically less than 10 μm). This means, for example, that it is not possible to apply standard ellipsometry techniques, which are commonly used for sensitive measurement of layer thicknesses and optical constants.[14,15] By contrast, imaging ellipsometry provides lateral resolution as low as 1 μm.[16] In this technique, a collimated incident beam is incident on the sample, and the illuminated sample surface is imaged onto a CCD camera using a microscope objective. High spatial resolution can thus be achieved while retaining accurate measurement of layer thicknesses and optical constants.

We therefore propose imaging ellipsometry as an effective tool for optical characterization of graphene oxide and similar materials, providing, in particular, information about changes in the optical properties of the material as a result of chemical or thermal reduction. These properties may subsequently be correlated with electronic behavior and chemical structure. We note that the measured optical properties are not those of an ideal, isolated sheet of graphene oxide but are, rather, the effective properties of the real material, including entrained water, adsorbed molecules, and interactions between the material and the substrate. The fitted values for effective index of refraction and extinction coefficient, and their changes after sample treatment, thus provide an important probe of the composite material's physical properties and their changes.

In this work, the effective optical properties and thicknesses of single and multiple layers of graphene oxide are characterized by imaging ellipsometry and compared with prior results obtained by confocal microscopy.[17] The effective optical dispersion parameters of a stack of graphene oxide sheets, approximately 100 nm thick, are measured by standard spectroscopic ellipsometry. From the dispersion parameters of such a multilayer stack, the dispersion parameters of individual graphene oxide sheets were determined according to an effective medium approximation. The effect of thermal treatment of graphene

* Corresponding author. Tel: (512) 471-4691. E-mail: r.ruoff@mail.utexas.edu.
[†] The University of Texas at Austin.
[‡] Nanofilm Technologie GmbH.
[§] Argonne National Laboratory.
[||] Northwestern University.

10.1021/jp802173m CCC: $40.75

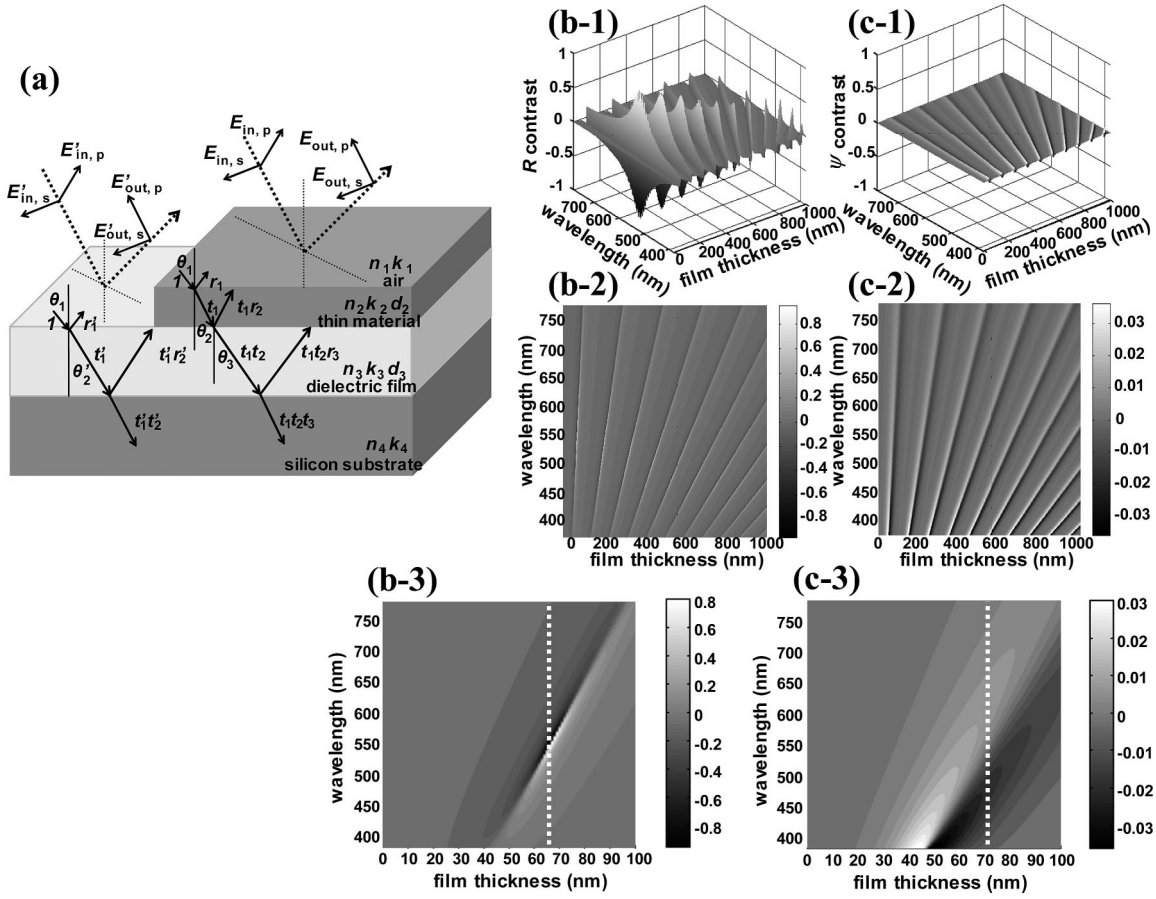

Figure 1. (a) Optical reflection and transmission for two incident polarizations from a layered thin-film system: dielectric film on silicon substrate (left side) and thin sheet on top of the dielectric film (right side). (b) Contrast from reflectance as a function of wavelength and film thickness with numerical aperture of illumination of 0.29: represented as three-dimensional plot (b-1), two-dimensional contour plot (b-2), and thickness range reduced (b-2). (c) Contrast from ellipsometric parameter (Ψ) at angle of incidence of 60° as a function of wavelength and film thickness: represented as three-dimensional plot (c-1), two-dimensional contour plot (c-2), and thickness range reduced (c-2). (Dotted lines on panels b-3 and c-3 represent thicknesses of dielectric film prepared for each test.)

oxide, which rendered the material electrically conductive, was investigated and explained by a simple model.

Theory

An ellipsometer measures the reflection of polarized light from a sample. Incident light is, in general, a superposition of the orthogonal s- and p-polarization components, $E_{in,s}$ and $E_{in,p}$, as illustrated in Figure 1a; similarly, the reflected light is a superposition of $E_{out,s}$ and $E_{in,s}$. The result of the ellipsometric measurement is the ratio of the amplitude reflection coefficients $r_s = E_{out,s}/E_{in,s}$ and $r_p = E_{out,p}/E_{in,p}$. This ratio is a complex number, defined as[11]

$$r_p/r_s = \tan \psi e^{i\Delta} \quad (1)$$

where $\psi = \tan^{-1}[|r_p|/|r_s|]$ and Δ is the phase difference between r_p and r_s. By fitting the measured values of Ψ and Δ, the optical properties and thickness (d) of the layer(s) are obtained.

The reflection coefficients can be calculated from the Fresnel reflection and transmission coefficients at each interface.[19–21] In the absence of a thin material layer, there are two interfaces, as illustrated in Figure 1a: between air and the dielectric layer, with Fresnel reflection coefficient r_1', and between the dielectric layer and the silicon substrate, with reflection coefficient r_2'. In this case, the total reflection coefficient is

$$r = (r_1' + r_2' \exp(-2i\delta_2'))/(1 + r_1'r_2' \exp(-2i\delta_2')) \quad (2)$$

where δ_2' is the phase change in the dielectric layer: $\delta_2' = d_3(n_3 - ik_3) \cos \theta_2' 2\pi/\lambda$. These values are all determined by the wavelength, λ, of the incident beam, the incident angle, θ, and the optical properties and thickness of each layer. Equation 2 is applicable for both polarizations.

When material is deposited on the substrate, it can be treated as a third layer added to the previous system. The total reflection coefficient is then

$$r = \frac{r_1 + r_2 \exp(-2i\delta_2) + [r_1r_2 + \exp(-2i\delta_2)]r_3 \exp(-2i\delta_3)}{1 + r_1r_2 \exp(-2i\delta_2) + r_3 \exp(-2i\delta_3)[r_2 + r_1 \exp(-2i\delta_2)]} \quad (3)$$

where r_1 is the amplitude of the light reflected at the interface between air and the thin layer of material, r_2 is the reflection between the thin layer of material and the dielectric layer, and r_3 is the reflection between the dielectric layer and the silicon layer. δ_2 and δ_3 are phase changes across the deposited material and dielectric layer, respectively: $\delta_2 = d_2(n_2 - ik_2) \cos \theta_2 2\pi/\lambda$, and $\delta_3 = d_3(n_3 - ik_3) \cos \theta_3 2\pi/\lambda$, where n_2 and k_2 are the effective index of refraction and absorption coefficient, respectively, for the thin material layer, and d_2 is its thickness.

We define the contrast of a parameter x by the Michelson contrast formulation[22]

$$\text{contrast}_x = (x_{material} - x_{dielectric})/(x_{material} + x_{dielectric}) \quad (4)$$

where $x_{material}$ represents optical parameters measured with the graphene-oxide layer present, and $x_{dielectric}$ represents values

measured on the dielectric film without the graphene-oxide layer. As optical parameters, ellipsometric parameters (Δ, Ψ) as well as reflectance (R) can be used.

Experimental Section

General. The substrates were prepared as follows. First, a dielectric film, silicon dioxide or silicon nitride, was grown on a silicon wafer (p-type, prime grade, (100) direction, from Helitek), and then 4 μm-square alignment marks were patterned on the surface. Graphene oxide sheets were then deposited on the substrate from an aqueous colloidal suspension, and the alignment marks were used to find the same area with a confocal microscope (Leica LCS laser confocal microscope SP2 system) and an AFM (Park Scientific AutoProbe CP/MT scanning probe microscope).

A PDMS mold was used as a mask for deposition of a multilayered film of graphene oxide ("graphene oxide stack"). The predeposited metal "scale" pattern was used as alignment marks for placing a PDMS mask, and later on, as a positioning reference for profilometer measurements (P-10, KLA Tencor, Inc.).

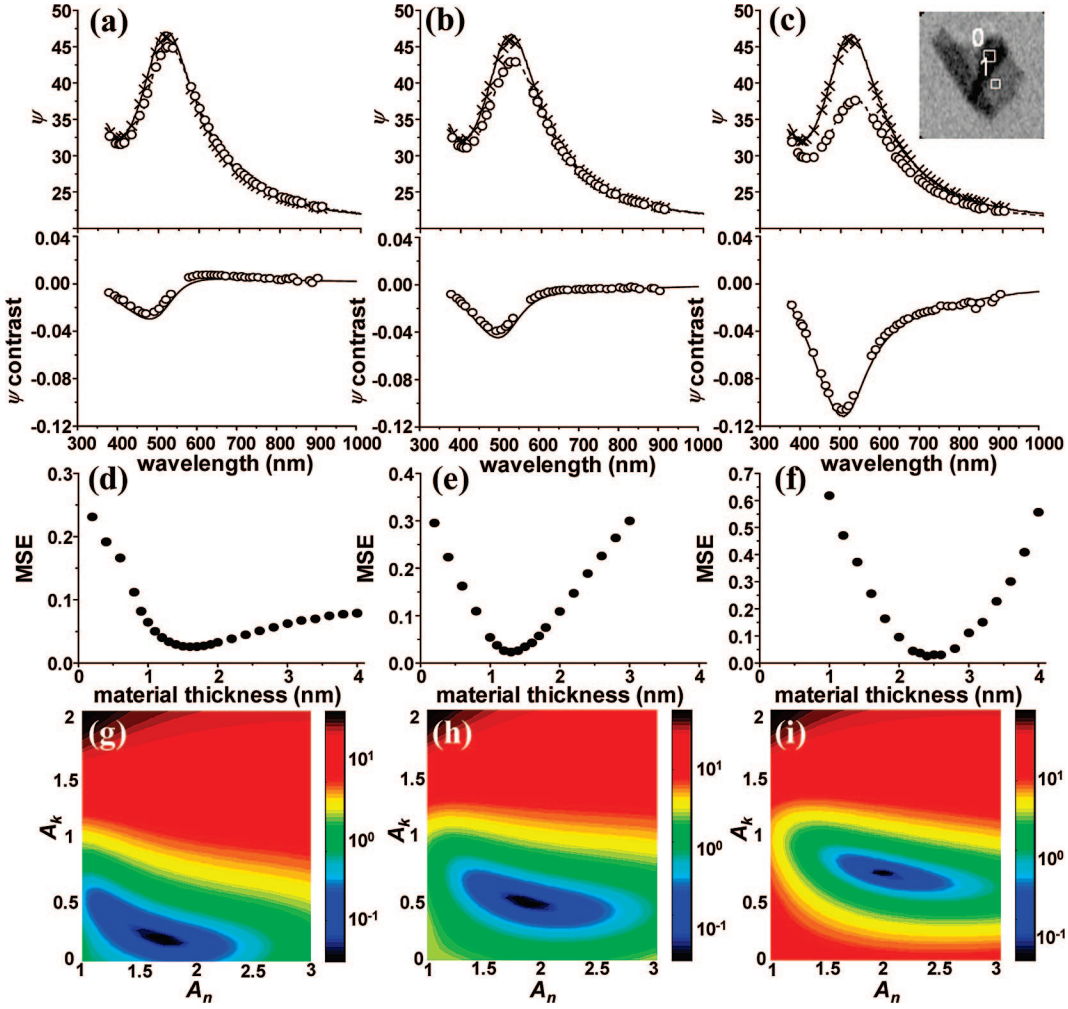

Figure 2. (a−c) Ellipsometric parameters for graphene oxide sheet: Ψ and Ψ-contrast for nonreduced single layer (a), thermally treated single layer (b), and thermally treated triple layer (c). The inset is the ellipsometric contrast image, size 50 μm × 50 μm, taken at a wavelength of 517 nm. Marked rectangles are regions of interest, over which Ψ is integrated. The area noted by "0" is on top of the triple layer and the area noted by "1" is a single layer. (d−f) The minimized value of MSE at the given material thickness which is varying from 0∼4 nm. (g−i) Contour maps of the MSE at fitted graphene-oxide thicknesses; A_n and A_k are coefficients of the Cauchy functions $n(\lambda) = A_n + B_n/\lambda^2$ and $k(\lambda) = A_k + B_k/\lambda^2$. The constant values B_n and B_k are assumed to be 3000 and 1500, respectively.

TABLE 1: Optical Properties and Thicknesses of Graphene Oxide Layers Determined by Fitting Data from Imaging Ellipsometry[a]

reduction treatment	number of layers	thickness (nm)		A_n	A_k
		fitted	measured		
not reduced	1	1.6 ± 0.8	1.25 ± 0.08	1.70 ± 0.30	0.18 ± 0.05
not reduced	1	1.7 ± 0.8	1.25 ± 0.08	1.71 ± 0.30	0.16 ± 0.05
reduced	1	1.3 ± 0.3	1.31 ± 0.10	1.87 ± 0.20	0.46 ± 0.07
reduced	3	2.4 ± 0.3	2.79 ± 0.14	1.99 ± 0.20	0.69 ± 0.07
reduced	1	1.3 ± 0.3	1.31 ± 0.10	1.87 ± 0.20	0.49 ± 0.07

[a] The first two cases are before thermal reduction and the lower three are after thermal reduction. As a comparison, thicknesses measured by AFM are included. A_n and A_k are coefficients of the Cauchy functions, $n = A_n + B_n/\lambda^2$ and $k = A_k + B_k/\lambda^2$. The values of the constants B_n and B_k are assumed to be 3000 and 1500, respectively.

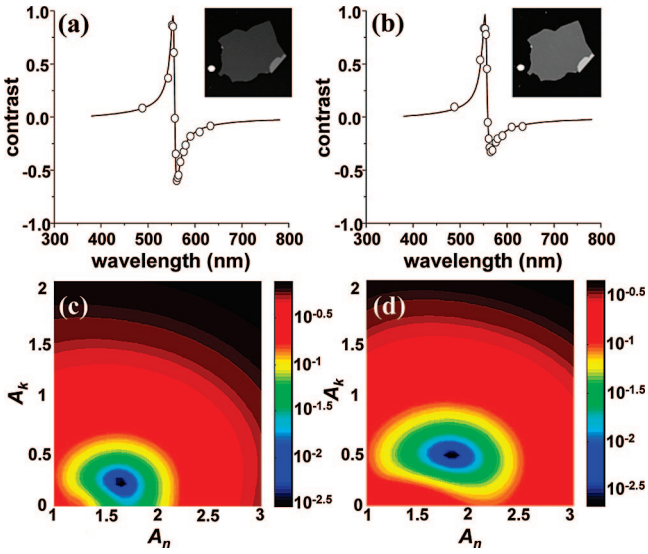

Figure 3. Contrast measured by variable wavelength confocal microscopy vs. wavelength of incident light; before (a) and after (b) thermal treatment, and calculated contrast (solid lines). Inset images are confocal microscope images at 543 nm before (left inset) and after (right inset) thermal treatment. Contour map of the MSE between the measured and the calculated contrast before (c) and after (d) thermal treatment.

Dielectric Film Growth on a Si Wafer. The SiO_2 thin film was grown by thermal oxidation (atmospheric oxidation furnace from Bruce Technologies, Inc., Nanotechnology Core Facility, University of Illinois at Chicago) with a furnace temperature of 1100 °C. The film thickness was later measured with a spectroscopic ellipsometer (MV-2000; J. A. Woolam, Inc.). The SiO_2 film thickness varied slightly across each wafer, such that the average thickness was 270 ± 10 nm. The surface roughness of the dioxide measured by AFM was 0.24 nm, which was less than the thickness of single layer graphene oxide (~1 nm). Silicon nitride was grown on silicon at the Cornell NanoScale Science & Technology Facility, using an LPCVD system. The average thickness of the film was 70 ± 10 nm. The surface roughness of the nitride measured by AFM was 0.27 nm.

Patterning of Alignment Marks. Squares 4 μm × 4 μm in size were patterned as alignment marks using an optical lithography system (MA6, Karl Suss, Inc.). In order to cover a large area of the substrate, the squares were patterned on the substrate in 10 × 10 blocks. A survey of distances separating the squares (30, 50, and 75 μm) was undertaken to find an intersquare separation that was compatible with the lateral dimensions of the graphene oxide sheets, and 50 μm was chosen. Ti (1 nm thick) followed by Au (2 nm thick) was then deposited, and the masked area was lifted off. Very thin Ti and Au were chosen in order to allow clear imaging with the confocal microscope. A quartz crystal monitor (XTM/2 Thin Film Deposition Monitor from Inficon) measured the thickness of the metal during deposition in the deposition system (Varian 3117 E-beam Evaporator).

Single-Layer and Multilayer Deposition. Prior to deposition of the graphene oxide material, prepared by the Hummers method,[3] the substrate was sonicated, first in acetone (VWR International, reagent grade) for 5 min and then in iso-propanol (J.T. Baker, reagent grade) for 3 min; nitrogen gas (Airgas, Inc.) was then blown over the surface to dry the substrate. Then the substrate was treated with oxygen plasma for 3 min in a plasma cleaner (Plasma Preen II-862 from Plasmatic systems, Inc.). This process makes the surface hydrophilic, so that the aqueous suspension of graphene oxide sheets would wet the surface well and a homogeneous dispersion of the graphene oxide sheets on the substrate could be achieved. To minimize the coverage of graphene oxide sheets deposited from the applied droplet, the as-prepared suspension was diluted 100-fold in deionized water (final concentration 0.01 mg/mL).[4] After a droplet was placed on the substrate, the substrate was blown with nitrogen gas before drying in air. The time between placing the droplet and blowing with N_2 (g) was varied so as to get sparsely dispersed material, and based on different trials, a delay of 1 min was chosen for sample preparation.

Thick-Stack Deposition. A thick stack of overlapping graphene oxide sheets was made using a PDMS mold as a deposition mask. The PDMS mold was made by mixing silicone elastomer base (Sylgard 184) and curing agent (from Dow Corning Corporation) in a 10:1 ratio (by mass). This mixture was poured on the silicon wafers, spun for 1 min at 500 rpm, and cured at 90 °C for 2 h. Circular holes of 3, 6, and 8 mm in diameter were made in a PDMS sheet using a micro punch (Harris Uni-Core from Whatman, Inc.). Because the PDMS material adheres well to the substrate and is hydrophobic, it worked as a mask for defining the region where a droplet of the aqueous colloidal suspension of the graphene oxide sheets would be deposited on the substrate. A concentration of 1 mg/mL of graphene oxide in water was used. A droplet was placed on the hydrophilic surface (previously prepared by oxygen plasma cleaning) and dried in ambient for 24 h.

Profilometry. To obtain a three-dimensional average topology of the graphene oxide stack deposited on a substrate by profilometry, markers indicating the starting positions of each profile were needed. Therefore, 5-mm-long markers with 100-μm spacing were patterned, and sample scanning with a profilometer (P-10; KLA Tencor, Inc.) was coordinated with these markers. To subtract the background profile, we used a custom written Matlab procedure applying a second-order polynomial regression. The three-dimensional topography of the graphene oxide stack was obtained by averaging 45 measured profiles.

Thermal Treatment. The deposited graphene oxide material was inserted in a vacuum furnace (Isotemp vacuum oven model 280A; Fischer Scientific), which was evacuated by a roughing pump (Duo seal vacuum pump from Welch Vacuum Technology, Inc., 1×10^{-4} Torr base pressure). The sample was inserted in the furnace at room temperature and pumped down, and the furnace temperature was ramped up to 200 °C in 1 h, held at 200 °C for 2 h, and then ramped down to room temperature in 4 h.

Spectroscopic Imaging Ellipsometry. A spectroscopic imaging ellipsometer (nulling ellipsometer EP3; Nanofilm Technologie GmbH, Goettingen, Germany) was used to measure the refractive index, extinction coefficient, and film thickness of single and multiple layers of graphene oxide sheets, with a 2 μm lateral resolution provided by a 10X microscope objective at 60° angle of incidence. The nulling ellipsometer measures the phase shift Δ and the ratio of reflection coefficients of p and s polarizations Ψ in four different ellipsometric zones.[15] The parameters Δ and Ψ are obtained as mean values of a "region of interest" (ROI). To obtain the best accuracy of ±0.05° in Ψ, the parameters Δ and Ψ were measured in all 4 ellipsometric zones and averaged. Data were fit to an optical model of the sample in which the dispersion of the graphene oxide was assumed to follow the Cauchy function $n(\lambda) = A_n + B_n/\lambda^2$ and $k(\lambda) = A_k + B_k/\lambda^2$ as a function of the wavelength λ, using typical values of $B_n = 3000$ nm^2 and $B_k = 1500$ nm^2.[18] First, the dielectric-layer thickness is determined by fitting the spectra of the background outside the perimeter of the graphene oxide sheets. This value is then used for fitting the thickness,

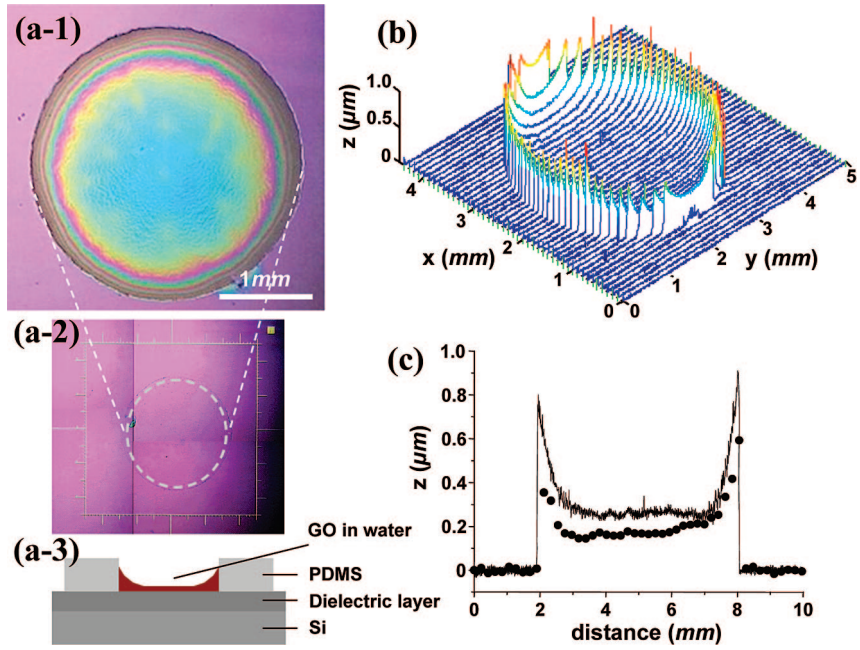

Figure 4. (a-1) Optical microscope image of a dried drop of graphene-oxide sheets, on a 266 nm thick silicon-dioxide layer on Si. (a-2) Reference scale patterns for profilometry measurement. The dotted circle is the area where graphene oxide is deposited. (a-3) Schematic of the deposition of a stack of graphene oxide sheets. (b) Three- dimensional topography of the stack as measured by a profilometer. (c) Thickness of a graphene-oxide stack before (solid line) and after (solid dots) thermal reduction.

refractive index A_n, and extinction A_k for the ROIs containing graphene oxide.

Spectroscopic Ellipsometry. To use the spectroscopic ellipsometer on the roughly 100-nm thick, 6-mm diameter stack of overlapping graphene oxide sheets, pinholes were used to reduce the beam size from the standard ≈2 mm to 0.5 mm diameter. Ellipsometry data were recorded before and after deposition of the graphene oxide multilayer stack and also after thermal treatment, and the optical properties and thickness of the multilayer stack were fitted by modeling with a Cauchy function.

AFM Thickness Measurement. AFM imaging (Park Scientific AutoProbe CP/MT scanning probe microscope) was used to obtain the thickness of the graphene oxide sheets. The targeted sheets could be found by comparing images from the confocal microscope with images from the optical microscope in the AFM. The thickness was determined by correcting for the nonuniform profile of the substrate.

Variable-Wavelength Confocal Microscope Imaging. Variable-wavelength confocal microscopy was performed using a home-built system. Incident light was produced by an optical parametric oscillator pumped by a mode-locked Ti:Sapphire laser (Coherent Mira), which has continuously tunable emission with a bandwidth of approximately 5 nm. This light was coupled into an inverted microscope (Olympus IX71), and focused with an objective (Olympus UPLAN APO 20×, numerical aperture = 0.7) on the sample surface. Reflected light from the sample was collected through the same objective and imaged on an optical fiber, which serves as the confocal aperture. The light coupled into the fiber was detected with a photomultiplier (Hamamatsu H5783), whose gain was adjusted for each image in order to maximize the signal-to-noise ratio while remaining in the linear regime of the detector. Images were obtained by scanning the sample over a 50 μm × 50μm region using a piezoelectric-driven flexure stage (Mad City Labs Nano-Bio2).

Results and Discussion

The values for the contrast of reflectance at normal incidence and of the ellipsometric parameter (Ψ) at an incidence angle of 60° are shown in Figure 1, panels b and c. For these calculations, silicon nitride was used as the dielectric film, the optical properties of the graphene oxide were assumed to be $n = 2$ and $k = 0$, and the thickness was fixed at 1 nm.[19] The contrast of reflectance oscillates between +0.8 to −0.8, but the ellipsometric parameter (Ψ) oscillates between only +0.03 and −0.03. The dotted lines in Figure 1, panels b-3 and c-3, represent the thicknesses of the dielectric layer prepared for measurement of reflectance as well as for imaging ellipsometry (67 and 71 nm, respectively). The Δ data obtained by imaging ellipsometry are not fitted in this work, since they have a small but important systematic error ±0.2°, due to optical anisotropy of the microscope objective in the imaging ellipsometer. This error means that fitting the data for Δ would reduce the accuracy of the fitted results as compared to fitting Ψ alone.

The measured spectroscopic imaging ellipsometric data for a single graphene oxide sheet before thermal treatment is shown in Figure 2a. The bottom curve of Figure 2a is the contrast of Ψ obtained directly from the upper curve. It shows a variation in the contrast as predicted from the simulation in Figure 1. The measured Ψ spectra are fitted by varying A_n, A_k, and d to minimize the mean-squared error (MSE), where

$$\mathrm{MSE} = \frac{1}{N}\sum_{i=1}^{N}\left(\psi_i^{\mathrm{mod}} - \psi_i^{\mathrm{exp}}\right)^2 \qquad (5)$$

A contour plot of MSE vs A_k and A_n is shown in Figure 2g. In Figure 2b, the measured spectroscopic ellipsometry data for a thermally treated single graphene oxide sheet is shown. In the contour plot of the MSE (Figure 2h), one sees that the effective optical properties are increased in comparison to the precursor graphene oxide material. For multiple layers of graphene oxide, the increases in A_n and A_k are larger than for the single-layer case. For example, the measured and calculated Ψ for a thermally treated trilayer are shown in Figure 2c. Compared with a single layer, the ellipsometric data have a larger difference from that of the bare substrate, as confirmed

by the contrast of the single layer and three layers, as shown in the inset image. In Table 1, the fitted values of the effective optical properties and thickness for five different graphene oxide samples are given.

The observed increase of the values of A_n and A_k after thermal reduction has previously been obtained by fitting the contrast of reflectance measured with a confocal microscope.[17] Compared with the ellipsometry results, the confocal-reflectivity method requires an independent measurement of the material thickness, since the MSE is not minimized as a function of thickness. In previous work, AFM measurements were used to determine the thickness and fit the reflectance data; here, we use instead the thicknesses obtained by fitting of ellipsometric data. In Figure 3, panels a and b, measured contrast as a function of the wavelength of the incident light is shown for graphene-oxide sheets before and after thermal treatment. The inset images, which were taken with a laser wavelength of 543 nm before and after the thermal treatment, show a clear increase of the contrast after thermal treatment. The MSE for single graphene-oxide layers by this method are shown in Figure 3, panels c and d. As in Figure 2, a distinct increase of A_n and A_k is seen. The average values of A_n and A_k for this single layer of graphene oxide before thermal treatment were determined to be 1.7 ± 0.3 and 0.17 ± 0.05, respectively, by ellipsometry, and 1.6 ± 0.2 and 0.2 ± 0.1, respectively, by confocal microscopy. After thermal treatment, the fitted values are 1.9 ± 0.2 and 0.47 ± 0.07 by ellipsometry, and 1.8 ± 0.2 and 0.4 ± 0.1 by confocal microscopy.[23] We note that ellipsometry gives reasonable fitting results, even though the contrast of Ψ is far lower than the contrast of reflectance, because of high accuracy in measuring Ψ and a low dependence of Ψ on the surface roughness (see the Supporting Information).

In an attempt to provide an additional measure and comparison of the optical properties of graphene oxide sheets, standard spectroscopic ellipsometry was used to characterize multilayer stacks of graphene oxide sheets. Note that these stacks are not "graphite oxide", which is a well-ordered and layered material made from graphite, but are instead a "reconstituted" multilayer material, similar to the "graphene oxide paper" that we have recently presented.[8] Figure 4b shows the topography of this graphene oxide stack, as measured by profilometry. The stack has a uniform thickness in its center and increased thickness at the perimeter, evidently due to a tendency to accumulate graphene oxide sheets at the edge as the droplet of the colloidal suspension dries. The thickness of the stack decreases after thermal treatment, as shown in Figure 4c. According to the profilometry measurements on 3-mm-diameter stacks, the average thickness of the flat center area was 260 nm before thermal treatment, and dropped to 170 nm after the thermal treatment, corresponding to a reduction of thickness of $34 \pm 5\%$.[24] Spectroscopic ellipsometery measurements on three 6-mm samples give a reduction in thickness of $42.3 \pm 5.5\%$.

These measurements also show an increase in the effective values of n and k of the graphene oxide stack after the thermal

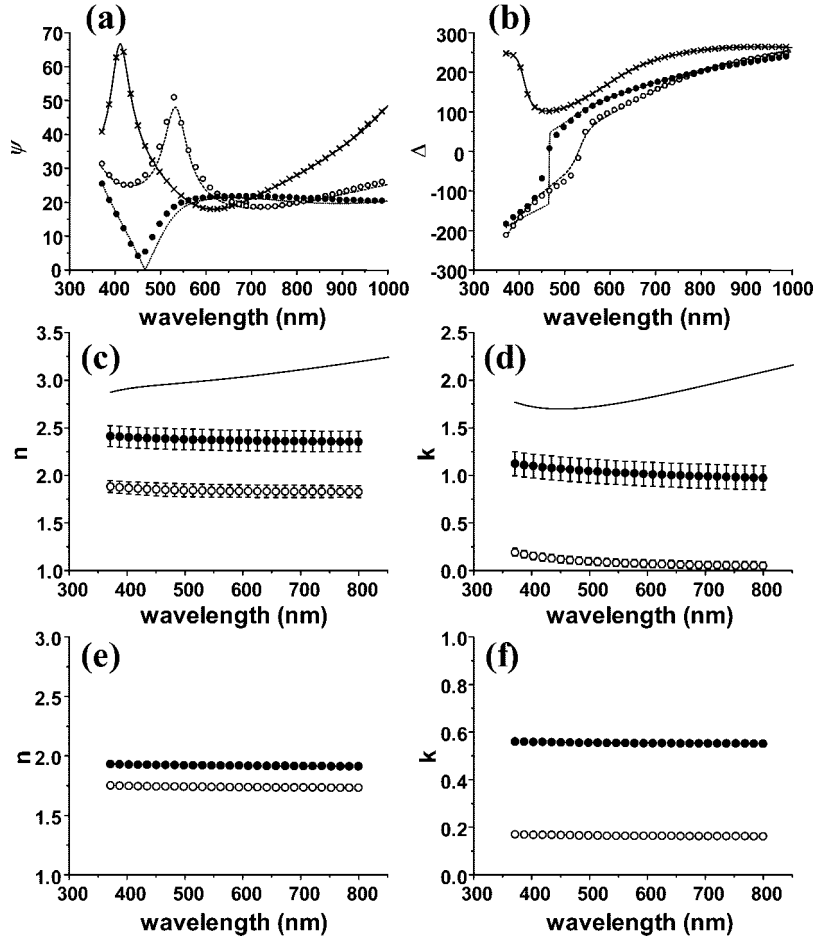

Figure 5. (a, b) Spectroscopic ellipsometry data of substrate (×), graphene-oxide stack before thermal treatment (○) and graphene-oxide stack after (●) thermal treatment. Solid lines are calculated values. (c, d) Optical properties of graphene oxide stack before (○) and after (●) thermal treatment and of highly oriented pyrolytic graphite pieces (—). Error bounds are the standard deviation over the four samples. (e, f) Optical properties of single and multiple layers of graphene oxide determined by imaging ellipsometry, before (○) and after (●) thermal treatment. Confidence intervals are shown in Table 1.

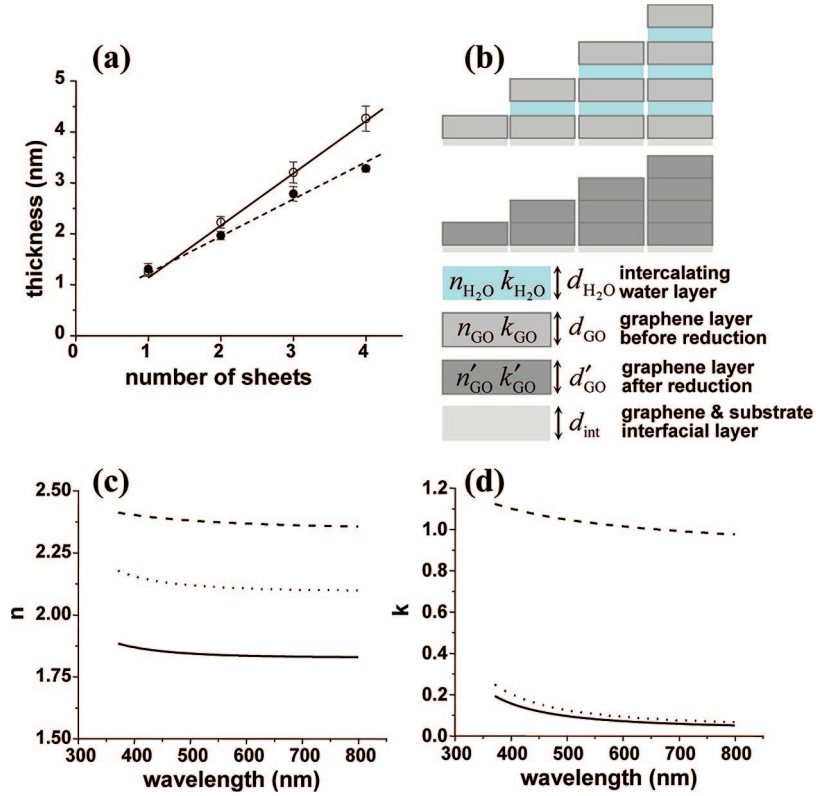

Figure 6. (a) Thickness vs number of sheets, before (○) and after (●) thermal treatment, as obtained by atomic-force microscopy. (b) Proposed model for thickness change by thermal reduction. (c, d) Optical properties found by fitting ellipsometry results for graphene-oxide stack before (solid line) and after (dashed line) thermal treatment, and the optical properties of the graphene-oxide layers alone, as determined by using an effective-medium approximation removing the effect of the interlamellar water layers (dotted line).

treatment. Four samples were measured; the average values and standard deviations are shown in Figure 5, panels c and d. When these optical constants are compared with values derived from measurements on a thick highly ordered pyrolytic graphite (HOPG) sample, the values for the thermally treated stack of graphene oxide sheets were found to be intermediate between that of graphite and the as-deposited stack. (The optical constants measured for the graphite sample agree with values obtained by EELS and published by others.[25]) As shown in Figure 5c−f, the increase of n and k for the multilayer graphene oxide stack following thermal treatment is greater than the increase found in the case of thermally treated single or multiple (but still thin) layers of graphene oxide sheets.

This result follows the trend previously reported for the optical constants of graphene, multilayer graphene, and graphite.[26,27] Others have rationalized the smaller values of n and k obtained for multilayer 'graphene' compared to bulk graphite as due to a possible decrease in interlayer interaction for a small number of layers.[28,29] Although this may also be the case for the thermally treated graphene oxide, the differences in optical constants may also be due to the influence of interlamellar water. Based on previous studies of graphene oxide stacks, one can infer that they are composed of layers of graphene oxide and interlamellar water.[8,29] The reduction in thickness upon heating can be explained as a change in the thickness of the interlamellar water. The total thickness before reduction can be expressed as $d = n\,(d_{GO} + d_{H_2O})$, where n is the number of layers, d_{GO} is the thickness of the as-deposited single layer of graphene oxide, and d_{H_2O} is the thickness of one layer of interlamellar water (all of them are assumed to be equal). After thermal treatment, the thickness changes to $d = n\,d_{GO}'$, where d_{GO}' is the thickness of a graphene-oxide layer after reduction. It should be noted that we here aim for qualitative understanding of the influence of changing the amount of interlamellar water in the multilayer stacks. Clearly, a significant amount of water is removed by heating in vacuum, although it is likely that some interlamellar water remains or is readsorbed after the sample is exposed to ambient.

For very thin multilayer stacks of graphene oxide, we employ a slightly different model. In Figure 6a, thicknesses are shown for up to four layers of graphene oxide. The reduction of thickness, if present, could not be measured for a single layer but is measurable for two or more layers. ("Anomalies" in the measured thicknesses of single layers have also been observed for graphene.[30]) From this finding, the modeled thickness can be slightly modified to describe thin stacks. The thickness of as-deposited very thin stacks is $d = d_{int} + d_{GO} + (n-1)\,(d_{GO} + d_{H_2O})$, and after a thermal treatment it is $d = d_{int}' + n\,d_{GO}'$, where d_{int} or d_{int}' is the thickness of the interfacial layer between the first layer of graphene oxide and the substrate before and after thermal treatment respectively.[31]

By using an effective medium approximation,[32] the effect of the water layer on the optical properties can be separated from the optical properties of the graphene oxide layers:

$$n_{GO\_wo\_H_2O} = \sqrt{\frac{n_{GO}^2 d_{GO} - n_{H_2O}^2 d_{H_2O}}{d_{GO\_wo\_H_2O}}},$$

$$k_{GO\_wo\_H_2O} = \sqrt{\frac{k_{GO}^2 d_{GO} - k_{H_2O}^2 d_{H_2O}}{d_{GO\_wo\_H_2O}}} \quad (7)$$

where $n_{GO\_wo\_H_2O}$, $k_{GO\_wo\_H_2O}$, and $d_{GO\_wo\_H_2O}$ are the optical properties and thickness of as-deposited graphene oxide layers alone, without the influence of the interlamellar water layers; n_{H_2O}, k_{H_2O}, and d_{H_2O} are the values for the interlamellar water layers; and n_{GO}, k_{GO}, and d_{GO} are the effective values for the

entire structure. Figure 6, panels c and d, show the optical properties of graphene oxide extracted using this model.[33] Accounting for the influence of the water layer yields a significantly increased value for n, but only a slightly increased value for k. From the above result, one can envision that the effect of thermal reduction is to remove interlamellar water layers, which results in the increase of index of refraction, and to reduce the oxygen content of graphene-oxide layers, which results in a significant increase of extinction coefficient.

Conclusions

The optical properties and thicknesses of single and multiple layers of graphene oxide were measured by an imaging ellipsometer. The measured optical properties were shown to increase by thermally treating the material in vacuum. Multiple layers of graphene oxide exhibited greater changes of optical properties than single layers. When conventional spectroscopic ellipsometry was applied to a stack of graphene oxide sheets, optical properties of the thermally reduced material were found to be much higher than the values for fewer layers, especially the index of refraction. As a consequence of thermal reduction, the thicknesses of multiple layers of graphene oxide reduced. Based on measured thicknesses before and after the thermal treatment, a model for the change in thickness was presented, in which some interlamellar water is removed. Using an effective medium approximation, the effect of the interlamellar water on the optical properties can be separated, and removal of interlamellar water can be shown to result in a significant increase in index of refraction. Developing a detailed understanding of the optical properties of individual and multilayer stacks of modified and unmodified graphene oxide platelets is of fundamental importance, adding to our understanding of the physical properties of these materials, and is also relevant to potential applications, such as transparent, flexible conductive films for photovoltaic and optoelectronic devices.

Acknowledgment. We thank Rob Ilic of the Cornell NanoScale Science & Technology Facility for the growth of silicon nitride film and Bob Lajos of Nanotechnology Core Facility at University of Illinois at Chicago for helping I.J. to grow the silicon dioxide film. We also thank Abel Thangawng for helping I.J. to preapre PDMS film and D. Gosztola for technical assistance with variable wavelength confocal microscopy. We gratefully acknowledge support from the DARPA Center on Nanoscale Science and Technology for Integrated Micro/Nano-Electromechanical Transducers (iMINT) (Award No: HR0011-06-1-0048). Work at the Center for Nanoscale Materials was supported by the U. S. Department of Energy, Office of Science, Office of Basic Energy Sciences, under Contract No. DE-AC02-06CH11357.

Supporting Information Available: Determination of the confidence interval and effect of the surface roughness. This material is available free of charge via the Internet at http://pubs.acs.org.

References and Notes

(1) Novoselov, K. S.; Geim, A. K.; Morozov, S. V.; Jiang, D.; Zhang, Y.; Dubonos, S. V.; Grigorieva, I. V.; Firsov, A. A. *Science* **2004**, *306*, 666.

(2) Novoselov, K. S.; Jiang, D.; Schedin, F.; Booth, T. J.; Khotkevich, V. V.; Morozov, S. V.; Geim, A. K. *Proc. Natl. Acad. Sci.* **2005**, *102*, 10451.

(3) Hummers, W.; Offeman, R. *J. Am. Chem. Soc.* **1958**, *80*, 1339.

(4) Stankovich, S.; Piner, R. D.; Chen, X.; Wu, N.; Nguyen, S. T.; Ruoff, R. S. *J. Mater. Chem.* **2006**, *16*, 155.

(5) Hirata, M.; Gotou, T.; Horiuchi, S.; Fujiwara, M.; Ohba, M. *Carbon* **2004**, *42*, 2929.

(6) Stankovich, S.; Dikin, D. A.; Dommett, G. H. B.; Kohlhaas, K. M.; Zimney, E. J.; Stach, E. A.; Piner, R. D.; Nguyen, S. T.; Ruoff, R. S. *Nature* **2006**, *442*, 282.

(7) Watcharotone, S.; Dikin, D. A.; Stankovich, S.; Piner, R.; Jung, I.; Dommett, G. H. B.; Evmenenko, G.; Wu, S.-E.; Chen, S.-F.; Liu, C.-P.; Nguyen, S. T.; Ruoff, R. S *Nano Lett.* **2007**, *7*, 1888.

(8) Dikin, D. A.; Stankovich, S.; Zimney, E. J.; Piner, R. D.; Dommett, G. H. B.; Evmenenko, G.; Nguyen, S. T.; Ruoff, R. S. *Nature* **2007**, *448*, 457.

(9) Li, Dan; Mueller, M. B.; Gilje, S.; Kaner, R. B.; Wallace, G. G. *Nat. Nanotechnol.* **2008**, *3*, 101.

(10) Gilje, S.; Han, S.; Wang, M.; Wang, K. L.; Kaner, R. B. *Nano Lett.* **2007**, *7*, 2758.

(11) Gomez-Navarro, C.; Weitz, R. T.; Bittner, A. M.; Scolari, M.; Mews, A.; Burghard, M.; Kern, K. *Nano Lett.* **2007**, *7*, 3499.

(12) Wang, X.; Zhi, L.; Muellen, K. *Nano Lett.* **2008**, *8*, 323–327.

(13) Eda, G.; Fanchini, G.; Chhowalla, M. *Nat. Nanotechnol.* **2008**, 83; Online publication doi:10.1038/nnano.

(14) Tompkins, H. G. *A User's Guide to Ellipsometry*; Academic Press: New York, 1993.

(15) Azzam, R. M.; Bashara, N. M. *Ellipsometry and Polarized Light*; North-Holland: Amsterdam, 1977.

(16) Beaglehole, D. *Rev. Sci. Instrum.* **1988**, *59*, 2557.

(17) Jung, I.; Pelton, M.; Piner, R.; Dikin, D.; Stankovich, S.; Watcharotone, S.; Hausner, M.; Ruoff, R. S *Nano Lett* **2007**, *7*, 3569.

(18) Palik, E. D., *Handbook of Optical Constants of Solids*, Academic Press, San Diego, 1998.

(19) Ward, L. *The Optical Constants of Bulk Materials and Films*; Institute of Physics publishing: Philadelphia, 1994.

(20) Macleod, H. A. *Thin-film Optical Filters*; American Elsevier Publishing Company Inc.: New York, 1969.

(21) Möller, K. D. *Optics*; University Science Books: Mill Valley, CA, 1988.

(22) Michelson, A. *Studies in Optics*; University of Chicago Press: Chicago, 1927.

(23) The method of determining confidence intervals of the fitted values from imaging ellipsometry is described in the supporting information. The error bounds of fitted values from confocal microscopy are described in the supporting information of ref 17. They are determined based on the assumption that the uncertainty of dielectric layer thickness and graphene oxide layer thickness are ± 0.2 nm respectively.

(24) The error bound of change in thickness by the profilometry measurement is determined by the nonuniformity of the profile. This is also expected to be the primary source of error in the ellipsometry measurements. The reported error bound of change in thickness by the ellipsometry measurement is determined by statistical analysis on three samples.

(25) Djurisic, A. B.; Li, E. H. *J. Appl. Phys.* **1999**, *85*, 7404.

(26) Blake, P.; Novoselov, K. S.; Castro Neto, A. H.; Jiang, D.; Yang, R.; Booth, T. J.; Geim, A. K.; Hill, E. W. *Appl. Phys. Lett.* **2007**, *91*, 063124.

(27) Ni, Z. H.; Wang, H. M.; Kasmin, J.; Fan, H. M.; Yu, T.; Wu, Y. H.; Feng, Y. P.; Shen, Z. X. *Nano Lett.* **2007**, *7*, 2758.

(28) Yoshizawa, K.; Yumura, T.; Yamabe, T.; Bandow, S. *J. Am. Chem. Soc.* **2000**, *122*, 11871–11875.

(29) Li, J. L.; Chun, J.; Wingreen, N. S.; Car, R.; Aksay, I. A.; Saville, D. A. *Phys. Rev. B* **2005**, *71*, 235412.

(30) Zhang, Y.; Tan, Y.; Stormer, H. L.; Kim, P. *Nature* **2005**, *438*, 201–204; online-supporting materials.

(31) It should be noted that the thickness change is larger in case for the multiple layers of graphene oxide than few layers, which is supposed to be due to relatively weak effect of the substrate for multiple layers.

(32) El-Haija, A. J. A. *J. Appl. Phys.* **2003**, *93*, 5.

(33) To be able to extract the thickness of the intercalating water layer from the compound layer (graphene oxide and intercalating water), we used the thickness of graphene oxide after thermal treatment. Because the purpose of the analysis is to check qualitatively the effect of the interlamellar water (at least, on that fraction that is removed by heating) on the optical properties of the whole system, we ignored the effect of any thickness reduction of graphene oxide itself.

JP802173M